J|A|C|S ARTICLES

Published on Web 09/16/2010

Glowing Locked Nucleic Acids: Brightly Fluorescent Probes for Detection of Nucleic Acids in Cells

Michael E. Østergaard,[†,§,⊥] Pallavi Cheguru,[‡,§,⊥] Madhusudhan R. Papasani,[‡,§] Rodney A. Hill,[*,‡,§] and Patrick J. Hrdlicka[*,†,§]

Department of Chemistry, University of Idaho, Moscow, Idaho 83844-2343, Department of Animal Veterinary Science, University of Idaho, Moscow, Idaho 83844-2330, and Biological Applications of Nanotechnology (BANTech) Center, University of Idaho, Moscow, Idaho 83844

Received July 9, 2010; E-mail: hrdlicka@uidaho.edu; rodhill@uidaho.edu

Abstract: Fluorophore-modified oligonucleotides have found widespread use in genomics and enable detection of single-nucleotide polymorphisms, real-time monitoring of PCR, and imaging of mRNA in living cells. Hybridization probes modified with polarity-sensitive fluorophores and molecular beacons (MBs) are among the most popular approaches to produce hybridization-induced increases in fluorescence intensity for nucleic acid detection. In the present study, we demonstrate that the 2′-*N*-(pyren-1-yl)carbonyl-2′-amino locked nucleic acid (LNA) monomer **X** is a highly versatile building block for generation of efficient hybridization probes and quencher-free MBs. The hybridization and fluorescence properties of these Glowing LNA probes are efficiently modulated and optimized by changes in probe backbone chemistry and architecture. Correctly designed probes are shown to exhibit (a) high affinity toward RNA targets, (b) excellent mismatch discrimination, (c) high biostability, and (d) pronounced hybridization-induced increases in fluorescence intensity leading to formation of brightly fluorescent duplexes with unprecedented emission quantum yields ($\Phi_F = 0.45-0.89$) among pyrene-labeled oligonucleotides. Finally, specific binding between messenger RNA and multilabeled quencher-free MBs based on Glowing LNA monomers is demonstrated (a) using *in vitro* transcription assays and (b) by quantitative fluorometric assays and direct microscopic observation of probes bound to mRNA in its native form. These features render Glowing LNA as promising diagnostic probes for biomedical applications.

Introduction

Homogeneous fluorescence-based assays for detection of nucleic acids[1] are widely used across the natural and life sciences, e.g., to detect single-nucleotide polymorphisms,[2] for real-time monitoring of PCR,[3,4] to study RNA folding,[5,6] and in the imaging of cellular RNA.[7−10] Development of fluorophore-modified oligonucleotides (ONs) for these purposes has accordingly been an area of intense focus.[11] Probes must produce measurable hybridization-induced differences in fluorescence intensity, as excess probe cannot be washed out.[12] Hybridization probes and molecular beacons (MBs) are the two probe strategies that have received the most attention toward this end.

Hybridization probes, i.e., ONs modified with a single kind of fluorophore, are designed to exhibit low fluorescence in the single-strand state through quenching of the fluorophore by neighboring nucleobases.[13,14] Hybridization with nucleic acid targets positions the fluorophore in a nonquenching microenvironment, leading to increased fluorescence emission. Examples include ONs labeled with Cy3,[15] fluorescein,[14,16,17] pyrene,[18−21] or base-discriminating fluorophores.[21−25]

The stem-loop structured MBs are typically end-labeled with fluorophore−quencher pairs.[26,27] Hybridization with nucleic acid

[†] Department of Chemistry.
[‡] Department of Animal and Veterinary Science.
[§] BANTech Center.
[⊥] These authors contributed equally.

(1) Ranasinghe, R. T.; Brown, T. *Chem. Commun.* **2005**, 5487–5502.
(2) Kim, S.; Misra, A. *Annu. Rev. Biomed. Eng.* **2007**, *9*, 289–320.
(3) Wilhelm, J.; Pingoud, A. *ChemBioChem* **2003**, *4*, 1120–1128.
(4) Kubista, M.; Andrade, J. M.; Bengtsson, M.; Forootan, A.; Jonak, J.; Lind, K.; Sindelka, R.; Sjoeback, R.; Sjoegreen, B.; Stroembom, L.; Zoric, N. *Mol. Aspects Med.* **2006**, *27*, 95–125.
(5) Bevilacqua, P. C.; Kierzek, R.; Johnson, K. A.; Turner, D. H. *Science* **1992**, *258*, 1355–1358.
(6) Smalley, M. K.; Silverman, S. K. *Nucleic Acids Res.* **2006**, *34*, 152–166.
(7) Bratu, D. P.; Cha, B.-J.; Mhlanga, M. M.; Kramer, F. R.; Tyagi, S. *Proc. Natl. Acad. Sci. U.S.A.* **2003**, *100*, 13308–13313.
(8) Silverman, A. P.; Kool, E. T. *Nucleic Acids Res.* **2005**, *33*, 4978–4986.
(9) Rodriguez, A. J.; Condeelis, J.; Singer, R. H.; Dictenberg, J. B. *Semin. Cell Dev. Biol.* **2007**, *18*, 202–208.
(10) Wu, Y.; Yang, C. J.; Moroz, L. L.; Tan, W. *Anal. Chem.* **2008**, *80*, 3025–3028.
(11) Asseline, U. *Curr. Org. Chem.* **2006**, *10*, 491–518.
(12) Seitz, O. In *Highlights in Bioorganic Chemistry: Methods and Applications*; Schmuck, C., Wennemers, H., Eds.; Wiley-VCH Verlag GmbH & Co.: Weinheim, 2004; pp 311−328.
(13) Manoharan, M.; Tivel, K. L.; Zhao, M.; Nafisi, K.; Netzel, T. L. *J. Phys. Chem.* **1995**, *99*, 17461–17472.
(14) Crockett, A. O.; Wittwer, C. T. *Anal. Biochem.* **2001**, *290*, 89–97.
(15) Randolph, J. B.; Wagonner, A. S. *Nucleic Acids Res.* **1997**, *25*, 2923–2929.
(16) Vaughn, C. P.; Elenitoba-Johnson, K. S. J. *Am. J. Pathol.* **2003**, *163*, 29–35.
(17) Dobson, N.; McDowell, D. G.; French, D. J.; Brown, L. J.; Mellor, J. M.; Brown, T. *Chem. Commun.* **2003**, 1234–1235.
(18) Yamana, K.; Iwase, R.; Furutani, S.; Tsuchida, H.; Zako, H.; Yamaoke, T.; Murakami, A. *Nucleic Acids Res.* **1999**, *27*, 2387–2392.
(19) Yamana, K.; Zako, H.; Asazuma, K.; Iwase, R.; Nakano, H.; Murakami, A. *Angew. Chem., Int. Ed.* **2001**, *40*, 1104–1106.

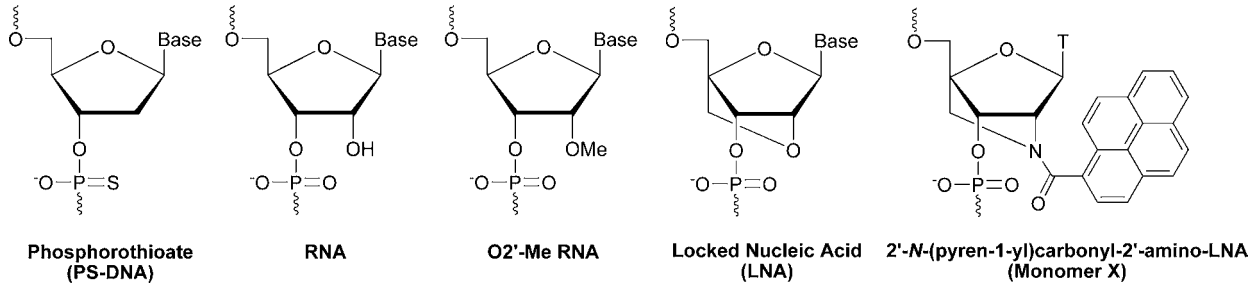

Figure 1. Structure of backbones and monomer **X** employed in this study.

targets leads to separation of the fluorophore−quencher pair and increased fluorescence intensity, which forms the basis of the widely used Sunrise[28] and Scorpion[29] primers. Among the chemical approaches to improve the biophysical characteristics of MBs,[27] fully modified locked nucleic acid (LNA) and LNA/DNA mixmer MBs have been reported.[10,30] Just like LNA-modified ONs,[31−35] these MBs display high target affinity and enzymatic stability,[30] enabling their use for RNA visualization in living cells over extended periods of time.[10] Following a different approach, *quencher-free MBs* have gained recent attention due to their straightforward probe design and ability for end-functionalization.[36] Introduction of microenvironment-sensitive fluorophores in the target recognition loop of quencher-free MBs has been a particularly promising approach toward nucleic acid recognition.[37−39]

Motivated by this and the ongoing interest in fluorophore-functionalized LNAs,[40−46] we recently developed DNA probes modified with 2′-*N*-(pyren-1-yl)carbonyl-2′-amino-LNA monomer **X** (Figure 1), which address several shortcomings exhibited by hybridization probes.[47] Thus, multilabeled 2′-*N*-(pyren-1-yl)carbonyl-2′-amino-LNAs result in specific formation of highly thermostable duplexes with complementary DNA/RNA targets, hybridization-induced increases in fluorescence intensity, and formation of brightly fluorescent duplexes with very high fluorescence emission quantum yields.[47] These characteristics have led others to coin the term "Glowing LNA" to these probes.[48] [Note: The terms "Glowing LNA" and "2′-*N*-(pyrene-1-yl)carbonyl-2′-amino-LNA" are used interchangeably and are defined as an ON (irrespective of backbone chemistry) containing one or more 2′-*N*-(pyrene-1-yl)carbonyl-2′-amino-2′-deoxy-2′-*N*,4′-*C*-methyleneribofuranosyl monomers.] Several analogues of monomer **X** have been prepared where the (pyren-1-yl)carbonyl moiety is either replaced with other fluorophores[40,41,49−51] or attached to a more flexible sugar ring.[52,53] Among these, 2′-*N*-(pyren-1-yl)carbonyl-2′-amino-LNA appears to most favorably combine structural and electronic features in a manner that leads to the above-mentioned characteristics irrespective of sequence contexts.[47]

In the present study, we set out to a) evaluate the importance of backbone chemistry on the hybridization and fluorescence properties of 2′-*N*-(pyren-1-yl)carbonyl-2′-amino-LNA monomer **X** (Figure 1), b) compare the detection ability of multilabeled hybridization probes and quencher-free MBs based on monomer **X** (Figure 2), and c) demonstrate the use of optimized Glowing LNA for detection of cellular RNA.

Results and Discussion

The corresponding phosphoramidite of 2′-*N*-(pyren-1-yl)carbonyl-2′-amino-LNA monomer **X** (Figure 1) was obtained as

(20) Korshun, V. A.; Stetsenko, D. A.; Gait, M. J. *J. Chem. Soc., Perkin Trans. 1* **2002**, *41*, 1092–1104.
(21) Østergaard, M. E.; Guenther, D. C.; Kumar, P.; Baral, B.; Deobald, L.; Paszczynski, A. J.; Sharma, P. K.; Hrdlicka, P. J. *Chem. Commun.* **2010**, *46*, 4929–4931.
(22) Okamoto, A.; Saito, Y.; Saito, I. *J. Photochem. Photobiol. C* **2005**, *6*, 108–122.
(23) Dodd, D. W.; Hudson, R. H. E. *Mini-Rev. Org. Chem.* **2009**, *6*, 378–391.
(24) Okamoto, A.; Kanatani, K.; Saito, I. *J. Am. Chem. Soc.* **2004**, *126*, 4820–4827.
(25) Bag, S. S.; Kundu, R.; Matsumoto, K.; Saito, Y.; Saito, I. *Bioorg. Med. Chem. Lett.* **2010**, *9*, 3227–3230.
(26) Tyagi, S.; Kramer, F. R. *Nat. Biotechnol.* **1996**, *14*, 303–308.
(27) Wang, K.; Tang, Z.; Yang, C. J.; Kim, Y.; Fang, X.; Li, W.; Wu, Y.; Medley, C. D.; Cao, Z.; Li, J.; Colon, P.; Lin, H.; Tan, W. *Angew. Chem. Int. Ed.* **2009**, *48*, 856–870.
(28) Nazarenko, I. A.; Bhatnager, S. K.; Hohman, R. J. *Nucleic Acids Res.* **1997**, *25*, 2516–2521.
(29) Whitcombe, D.; Theaker, J.; Guy, S. P.; Brown, T.; Little, S. *Nat. Biotechnol.* **1999**, *17*, 804–807.
(30) Yang, C. J.; Wang, L.; Wu, Y.; Kim, y.; Medley, C. D.; Lin, H.; Tan, *Nucleic Acids Res.* **2007**, *35*, 4030–4041.
(31) Singh, S. K.; Nielsen, P.; Koshkin, A. A.; Wengel, J. *Chem. Commun.* **1998**, 455–456.
(32) Wengel, J. *Acc. Chem. Res.* **1999**, *32*, 301–310.
(33) Petersen, M.; Wengel, J. *Trends Biotechnol.* **2003**, *21*, 74–81.
(34) Obika, S.; Uneda, T.; Sugimoto, T.; Nanbu, D.; Minami, T.; Doi, T.; Imanishi, T. *Bioorg. Med. Chem.* **2001**, *9*, 1001–1011.
(35) Kaur, H.; Babu, B. R.; Maiti, S. *Chem. Rev.* **2007**, *107*, 4672–4697.
(36) Venkatesan, N.; Seo, Y. J.; Kim, B. H. *Chem. Soc. Rev.* **2008**, *37*, 648–663.
(37) Hwang, G. T.; Seo, Y. J.; Kim, B. H. *J. Am. Chem. Soc.* **2004**, *126*, 6528–6529.
(38) Marti, A. A.; Jockusch, S.; Li, Z.; Ju, J.; Turro, N. J. *Nucleic Acids Res.* **2006**, *34*, e50.
(39) Ryu, J. H.; Seo, Y. J.; Hwang, G. T.; Lee, J. Y.; Kim, B. H. *Tetrahedron* **2007**, *63*, 3538–3547.
(40) Hrdlicka, P. J.; Babu, B. R.; Sørensen, M. D.; Wengel, J. *Chem. Commun.* **2004**, 1478–1479.
(41) Umemoto, T.; Hrdlicka, P. J.; Babu, B. R.; Wengel, J. *ChemBioChem* **2007**, *8*, 2240–2248.
(42) Lindegaard, D.; Madsen, A. S.; Astakhova, I. V.; Malakhov, A. D.; Babu, B. R.; Korshun, V. A.; Wengel, J. *Bioorg. Med. Chem.* **2008**, *16*, 94–99.
(43) Kumar, T. S.; Wengel, J.; Hrdlicka, P. J. *ChemBioChem* **2007**, *8*, 1122–1125.
(44) Kumar, T. S.; Madsen, A. S.; Østergaard, M. E.; Wengel, J.; Hrdlicka, P. J. *J. Org. Chem.* **2008**, *73*, 7060–7066.
(45) Kumar, T. S.; Madsen, A. S.; Østergaard, M. E.; Sau, S. P.; Wengel, J.; Hrdlicka, P. J. *J. Org. Chem.* **2009**, *74*, 1070–1081.
(46) Sau, S. P.; Kumar, T. S.; Hrdlicka, P. J. *Org. Biomol. Chem.* **2010**, *8*, 2028–2036.
(47) Hrdlicka, P. J.; Babu, B. R.; Sørensen, M. D.; Harrit, N.; Wengel, J. *J. Am. Chem. Soc.* **2005**, *127*, 13293–13299.
(48) Auld, D.; Simeonov, A. *Assay Drug Dev. Technol.* **2005**, *3*, 581–593.
(49) Astakhova, I. V.; Korshun, V. A.; Wengel, J. *Chem. Eur. J* **2008**, *14*, 11010–11026.
(50) Astakhova, I. V.; Korshun, V. A.; Jahn, K.; Kjems, J.; Wengel, J. *Bioconjugate Chem.* **2008**, *19*, 1995–2007.
(51) Gupta, P.; Langkjær, N.; Wengel, J. *Bioconjugate Chem.* **2010**, *21*, 513–520.
(52) Dohno, C.; Saito, I. *ChemBioChem* **2005**, *6*, 1075–1081.
(53) Honcharenko, D.; Zhou, C.; Chattopadhyaya, J. *J. Org. Chem.* **2008**, *73*, 2829–2842.

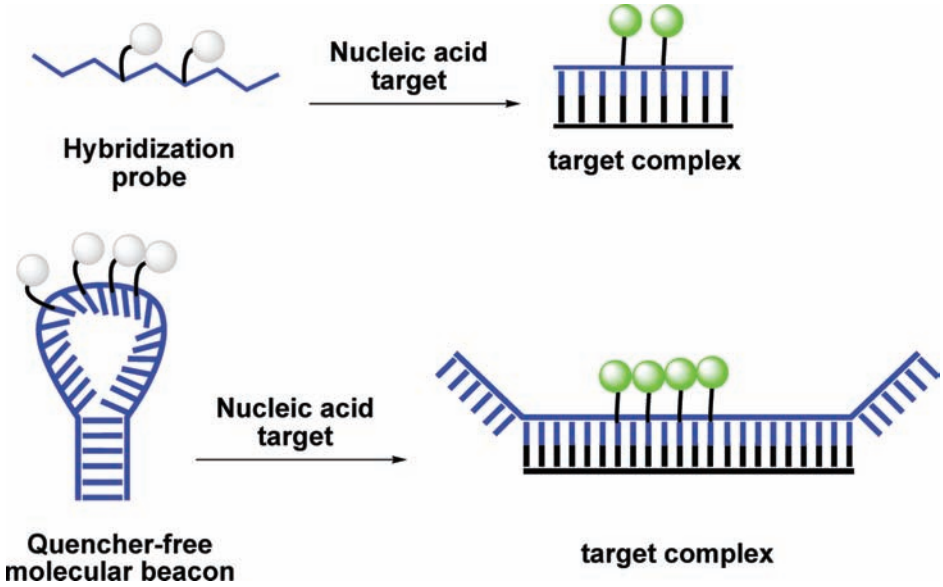

Figure 2. Principle of Glowing LNA used as multilabeled hybridization probes (upper) or multilabeled quencher-free molecular beacons (lower). Low levels of fluorescence are observed for single-stranded probes/regions due to nucleobase-mediated quenching of pyrene fluorescence, while dequenching occurs upon target hybridization, resulting in high levels of fluorescence.

Table 1. Sequences and MALDI-MS Analysis of Probes Used in This Study[a]

ON	sequence	*m/z* [M − H]$^-$ exptl	*m/z* [M − H]$^-$ calcd
DNA 1X	5′-d(GCA TA**X** CAC)	2938[b]	2937[b]
DNA 2X	5′-d(GCA **X**A**X** CAC)	3191[b]	3192[b]
PS-DNA 1X	5′-[PS-DNA]-(GCA TA**X** CAC)	3066	3066
PS-DNA 2X	5′-[PS-DNA]-(GCA **X**A**X** CAC)	3319	3321
RNA 1X	5′-r(GCA UA**X** CAC)	3052	3052
RNA 2X	5′-r(GCA **X**A**X** CAC)	3305	3304
O2′-Me RNA 1X	5′-[2′-OMe RNA]-(GCA UA**X** CAC)	3162	3163
O2′-Me RNA 2X	5′-[2′-OMe RNA]-(GCA **X**A**X** CAC)	3401	3402
LNA 1X	5′-[LNA]-(G^{Me}CA TA**X** ^{Me}CA^{Me}C)	3204	3204
LNA 2X	5′-[LNA]-(G^{Me}CA **X**A**X** ^{Me}CA^{Me}C)	3431	3432
DNA LP	5′-d(CCT T**X**A **X**C**X** G**X**T GCT)	5517	5517
DNA MB	5′-d(C GCT CGA CCT T**X**A **X**C**X** G**X**T GCT TCG AGC G)	9847	9848
O2′-Me RNA LP	5′-[2′-OMe RNA]-(CCU U**X**A **X**C**X** G**X**U GCU)	5797[c]	5795
O2′-Me RNA MB	5′-[2′-OMe RNA]-(C GCU CGA CCU U**X**A **X**C**X** G**X**U GCU UCG AGC G)	10501	10508

[a] For structures of backbones and monomer **X**, see Figure 1. ^{Me}C denotes 5-methylcytosin-1-yl. [b] Reported in ref 47. [c] Run in positive mode.

previously described.[54] Monomer **X** was incorporated into PS-DNA, RNA, O2′-Me RNA, or LNA strands (Figure 1), as these backbone chemistries are known to increase affinity toward nucleic acid targets,[31,55] improve binding specificity,[55,56] increase nuclease resistance,[57−60] and/or promote pyrene−nucleobase quenching in single-stranded probes (SSPs).[18,19] Automated synthesis of modified DNA, PS-DNA, RNA, O2′-Me RNA, and LNA probes was performed on a 0.2 μmol scale using typical conditions for these backbone chemistries, with the exception of extended coupling times during incorporation of monomer **X** (DNA/PS-DNA/LNA, 10/20/10 min using 1*H*-tetrazole; RNA/O2′-Me RNA, 15 min using pyridinium hydrochloride; see Supporting Information). These conditions resulted in coupling yields of >97% for monomer **X**. The identity and purity of the resulting ONs were verified by MALDI-MS analysis (Table 1) and ion-exchange HPLC (>80%), respectively (see Supporting Information).

Monomer **X** was first evaluated in an AT/AU-rich 9-mer that was identified as a particularly challenging sequence context in our initial studies, and which results in less pronounced hybridization-induced increases in fluorescence intensity.[47] This sequence context is therefore well-suited to identify probe backbones with improved hybridization and fluorescence properties. Singly modified DNA, PS-DNA, RNA, and O2′-Me RNA probes display markedly increased thermal affinity toward complementary DNA/RNA relative to the corresponding reference strands (see **1X** probes, ΔT_m/mod = +3.0 to +7.5 °C, Table 2). **DNA 1X** and **PS-DNA 1X** exhibit particularly stabilizing effects on duplexes with RNA complements. Incorporation of an additional **X** monomer as a next-nearest neighbor results in synergistic increases in duplex thermostability. [The

(54) Sørensen, M. D.; Pedersen, M.; Wengel, J. *Chem. Commun.* **2003**, 2130–2131.
(55) Majlessi, M.; Nelson, N. C.; Becker, M. M. *Nucleic Acids Res.* **1998**, *26*, 2224–2229.
(56) You, Y.; Moreira, B. G.; Behlke, M. A.; Owczarzy, R. *Nucleic Acids Res.* **2006**, *34*, e60.
(57) Stein, C. A.; Subasinghe, C.; Shinozuka, K.; Cohen, J. S. *Nucleic Acids Res.* **1988**, *16*, 3209–3221.
(58) Hoke, G. D.; Draper, K.; Freier, S. M.; Gonzalez, C.; Driver, V. B.; Zounes, M. C.; Ecker, D. J. *Nucleic Acids Res.* **1991**, *19*, 5743–5748.
(59) Sproat, B. S.; Lamond, A. I.; Beijer, B.; Neuner, P.; Ryder, U. *Nucleic Acids Res.* **1989**, *17*, 3373–3386.
(60) Frieden, M.; Christensen, S. M.; Mikkelsen, N. D.; Rosenbohm, C.; Thrue, C. A.; Westergaard, M.; Hansen, H. F.; Ørum, H.; Koch, T. *Nucleic Acids Res.* **2003**, *31*, 6365–6372.

Table 2. Thermal Denaturation Temperatures (T_m) and Fluorescence Quantum Yields (Φ_F) of **1X** and **2X** Probes and Their Duplexes with DNA and RNA Complements[a]

	T_m (ΔT_m/mod)/°C		quantum yield (Φ_F)		
probe	+DNA	+RNA	SSP	+DNA	+RNA
DNA 1X[b]	32.5 (+3.0)	33.0 (+6.0)	0.50	0.79	0.91
DNA 2X[b]	40.5 (+5.5)	41.5 (+7.5)	0.27	0.81	0.70
PS-DNA 1X	24.0 (+3.5)	26.0 (+7.5)	0.50	0.64	0.66
PS-DNA 2X	32.0 (+6.0)	35.0 (+8.5)	0.20	0.61	0.62
RNA 1X	31.5 (+4.5)	42.5 (+4.5)	0.84	0.89	0.93
RNA 2X	38.0 (+5.5)	46.5 (+4.0)	0.16	0.85	0.89
O2′-Me 1X	31.0 (+5.0)	45.0 (+4.5)	1.00	0.97	0.98
O2′-Me 2X	20.0[c] (−3.0)	46.0 (+3.0)	0.14	0.68	0.86
LNA 1X	54.5 (−3.5)	64.0 (−5.0)	0.95	0.90	0.89
LNA 2X	49.0 (−4.5)	60.5 (−4.5)	0.72	0.92	0.84

[a] Each strand used at 1.0 μM. Thermal denaturation buffer: 110 mM NaCl, 0.1 mM EDTA, pH 7.0 adjusted with 10 mM NaH_2PO_4/5 mM Na_2HPO_4. For probe sequences, see Table 1. ΔT_m/mod values determined relative to corresponding unmodified reference strands. Quantum yields determined at 5 °C. [b] Values taken from ref 47. [c] Determined at 250 nm (Figure S3). T_m value was verified by steady-state fluorescence emission spectroscopy (Figure S4) and using different batches of **O2′-Me 2X**; see Supporting Information.

puzzling behavior of the duplex between **O2′-Me RNA 2X** and cDNA is discussed in the Supporting Information.] The LNA-based probes deviate from these trends, as incorporation of **X** monomers results in progressively decreased thermal affinity toward DNA/RNA targets relative to the corresponding LNA reference strand (Table 2). This simply reflects the fact that a LNA thymine monomer is more stabilizing than most corresponding N2′-functionalized 2′-amino-LNA derivatives.[54] Within the context of cellular RNA imaging, it is interesting to note that the thermostability of duplexes between 2′-*N*-(pyren-1-yl)carbonyl-2′-amino-LNA probes and RNA targets increases in the following backbone-dependent order: PS-DNA < DNA < RNA ~ O2′-Me RNA < LNA (Table 2).

Steady-state fluorescence emission spectra (λ_{em} = 360−600 nm) and cross-calibrated fluorescence emission quantum yields (Φ_F) were obtained for SSPs and the corresponding duplexes with DNA/RNA targets at 5 °C (see Supporting Information). An excitation wavelength of λ_{ex} = 340 nm was chosen as the pyrene fluorophore exhibits prominent absorbance in this region, while low experimental temperatures were chosen to maximize strand hybridization. Two unstructured pyrene monomer emission peaks at $\lambda_{em} \approx$ 389 and 403 nm were observed for the duplexes, although minor backbone-specific variations in the location of emission maxima were observed (Figure 3; Figures S5−S12, Supporting Information).

Singly modified SSPs as well as the corresponding duplexes with DNA/RNA targets exhibit fluorescence emission quantum yields approaching unity (Table 2). Accordingly, only minor changes in fluorescence intensity were generally observed upon hybridization of **1X** probes with DNA/RNA complements (Figure 4, left). Interestingly, hyperchromicity of pyrene absorption was observed upon duplex formation (results not shown), leading to more pronounced hybridization-induced increases in fluorescence intensity than would be expected from comparison of emission quantum yields alone. [The "fluorescence brightness" of a species, i.e., the area under an emission spectrum, is linked to the fluorescence emission quantum yield Φ_F and the extinction coefficient of the fluorophore at the applied excitation wavelength (FB = $\Phi_F \varepsilon_{ex}$), while the "fluorescence intensity" describes the level of fluorescence at a given emission wavelength. **PS-DNA 1X** exhibits particularly prominent hyperchromicity.] Significantly lower quantum yields are observed for doubly modified SSPs (except **LNA 2X**), which most likely reflects increased quenching interactions between pyrene and nucleobase moieties. The corresponding duplexes between **2X** probes and DNA/RNA complements, however, remain brightly fluorescent (Φ_F = 0.61−0.89, Table 2). Interestingly, the differences in quantum yields between SSPs and duplexes with DNA/RNA complements are larger for **RNA 2X** and **O2′-Me RNA 2X** probes than for **DNA 2X** and **PS-DNA 2X** probes (Table 2). Thus, more pronounced increases in fluorescence intensity at $\lambda_{em} \approx$ 403 nm are observed upon hybridization of **RNA 2X** or **O2′-Me RNA 2X** to DNA/RNA complements (7.2/6.4- and 8.3/11.6-fold, respectively) than with **PS-DNA 2X** or **DNA 2X**[47] (4.5/4.6- and 3.3/3.2-fold, respectively) (Figure 4, right). These observations are in agreement with our initial studies on 2′-*N*-(pyren-1-yl)carbonyl-2′-amino-LNA in DNA backbones, which revealed that successful probe design necessitates incorporation of two or more separated **X** monomers to facilitate pyrene−nucleobase quenching in SSPs.[47] Molecular modeling studies suggested that the very high duplex quantum yields are a consequence of the conformationally locked bicyclic skeleton and the short amide linkage of monomer **X**, which precisely positions the fluorophore in the minor groove of duplexes and thereby minimizes quenching interactions between pyrene and nucleobase moieties.[13,47]

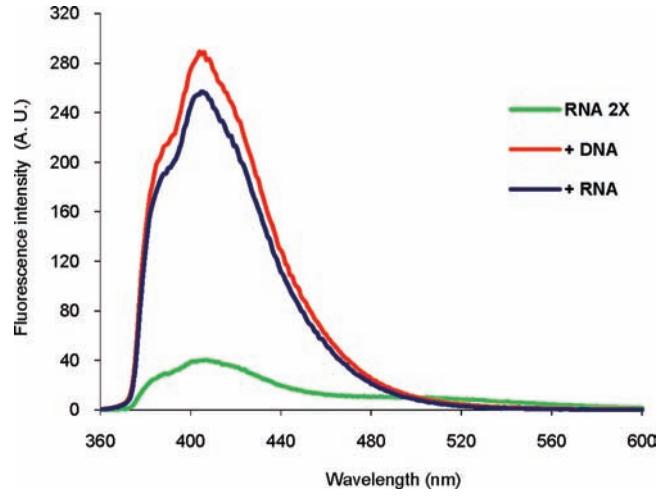

Figure 3. Fluorescence emission spectra of single-strand **RNA 2X** and the corresponding duplex with DNA or RNA, T = 5 °C, λ_{ex} = 340 nm.

In contrast, the **LNA 2X** probe exhibits very high SSP fluorescence, and only marginal hybridization-induced increases in fluorescence intensity are accordingly observed (Figure 4, right). We speculate that this is related to known rigidity of single-strand LNA,[61,62] whereby quenching interactions between pyrene and nucleobase moieties are reduced.

Next, the thermal discrimination of DNA/RNA strands with a centrally positioned mismatch was studied using the optimized **2X** probe designs (Table 3 and Table S1, Supporting Information). **PS-DNA 2X** and **LNA 2X** probes exhibit comparable or

(61) Petersen, M.; Nielsen, C. B.; Nielsen, K. E.; Jensen, G. A.; Bondensgaard, K.; Singh, S. K.; Rajwanshi, V. K.; Koshkin, A. A.; Dahl, B. M.; Wengel, J.; Jacobsen, J. P. *J. Mol. Recognit.* **2000**, *13*, 44–53.
(62) Konorov, S. O.; Schulze, H. G.; Addison, C. J.; Haynes, C. A.; Blades, M. W.; Turner, R. F. B. *J. Raman Spectrosc.* **2009**, *40*, 1162–1171.

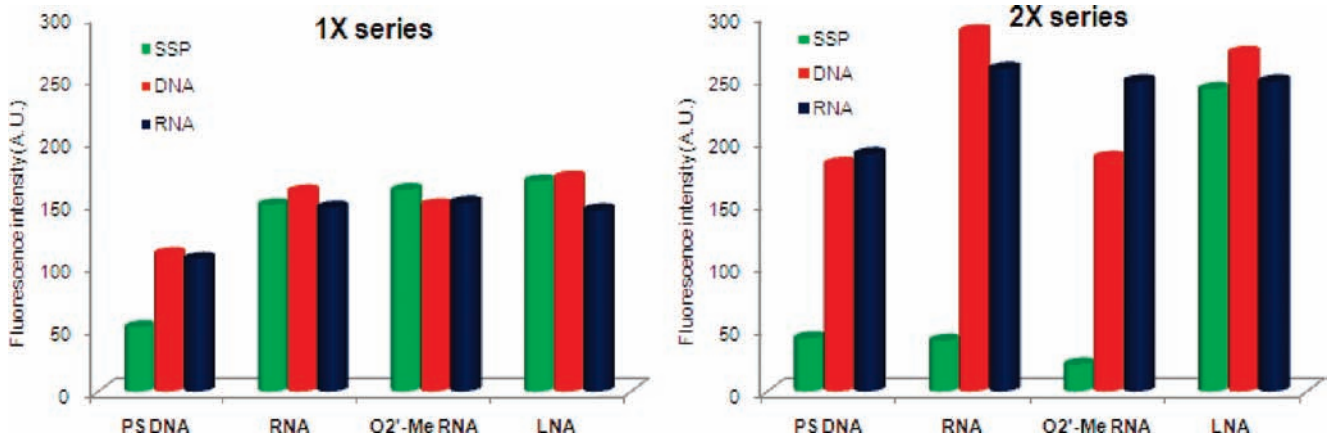

Figure 4. Fluorescence intensity of single-strand probes (SSPs) and corresponding duplexes with complementary DNA and RNA: left panel, **1X** probes; right panel, **2X** probes. Intensity observed at I_3 emission maximum using $\lambda_{ex} = 340$ nm at $T = 5$ °C. Concentration of each strand is 1.0 μM.

Table 3. Thermal Discrimination of DNA/RNA Targets with Central Mismatches by **2X** Probes[a]

		DNA: 3′-d(CGT AMA GTG)				RNA: 3′-r(CGU AMA GUG)			
		T_m	ΔT_m			T_m	ΔT_m		
probe	M =	T	A	C	G	U	A	C	G
DNA 2X[b]		**40.5**	−21.0	−15.5	−17.5	**41.5**	−14.5	−15.5	−10.5
PS-DNA 2X		**32.0**	−17.5	−16.5	−17.5	**35.0**	−17.5	−14.5	−13.0
RNA 2X[c]		**38.0**	< −28.5	< −28.0	< −28.0	**46.5**	−21.5	−21.0	−17.5
O2′-Me 2X[c]		**20.0**	< −10.0	< −10.0	< −10.0	**46.0**	−30.0	−26.0	−24.0
LNA 2X		**49.0**	−20.5	−21.5	−21.0	**60.5**	−16.5	−16.0	−15.5

[a] T_m values for duplexes with matched targets shown in bold. ΔT_m is the change in the T_m value relative to that of the fully matched duplex. [b] Values taken from ref 47. [c] No hyperchromicity was observed with mismatched DNA targets at 250 nor 260 nm, and fluorescence spectra also did not suggest duplex formation.

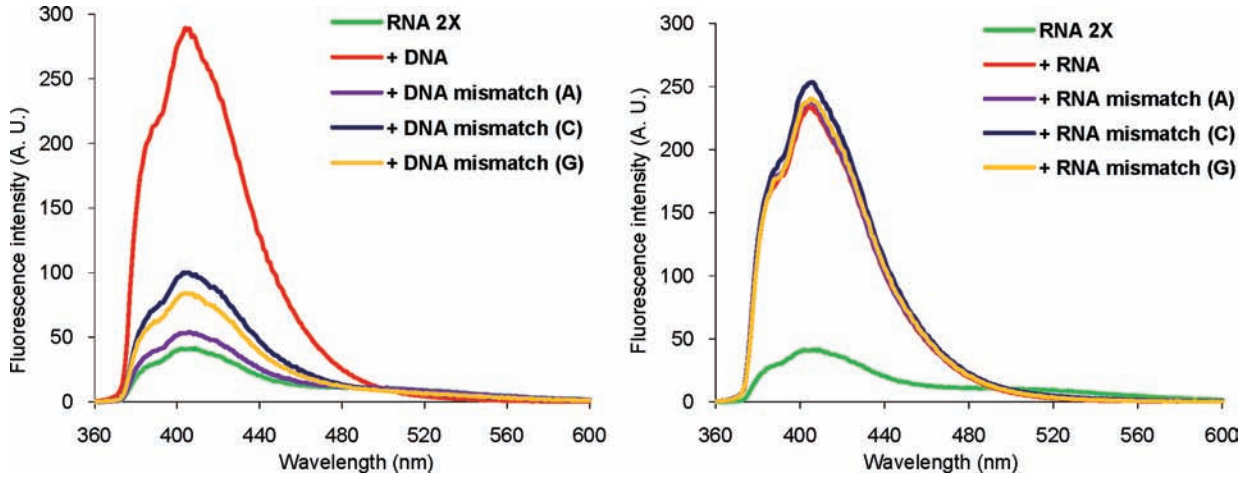

Figure 5. Steady-state fluorescence emission spectra of **RNA 2X** in the absence or presence of complementary or mismatched DNA (left) or RNA (right) strands (letter in parentheses denotes the centrally positioned mismatched nucleotide). All fluorescence spectra were recorded at 5 °C.

slightly improved mismatch discrimination relative to the original **DNA 2X** probe,[47] while **RNA 2X** and **O2′-Me RNA 2X** probes display extraordinary improvements (Table 3; also see Supporting Information). For example, the thermostability of duplexes between mismatched RNA targets and **DNA 2X** is only lowered by 10.5−15.5 °C relative to the matched duplex, while it is decreased by 17.5−21.5 or 24.0−30.0 °C when **RNA 2X** or **O2′-Me RNA 2X** is used, respectively.

The marked *thermal discrimination* of mismatched targets displayed by **RNA 2X** or **O2′-Me RNA 2X** probes can potentially reduce false positive signals in bioassays and enable *optical discrimination* of mismatched targets. For example, very low levels of emission are observed when spectra are recorded for **PS-DNA 2X**, **RNA 2X**, or **O2′-Me RNA 2X** at 5 °C in the presence of mismatched DNA targets, while the corresponding duplexes with complementary DNA are highly emissive (Figure 5, left; Figures S13−S15, Supporting Information). However, probes forming highly thermostable mismatched duplexes still emit bright fluorescence since the fluorophore is positioned in a similar microenvironment as in matched duplexes (see, e.g., **RNA 2X** vs RNA mismatches, Figure 5, right; Figure S16, Supporting Information). Thus, Glowing LNA probes rely on efficient thermal discrimination of mismatched targets to ensure optical discrimination, which is typical for hybridization probes.

Table 4. Thermal Denaturation Temperatures (T_m) and Fluorescence Emission Quantum Yields (Φ_F) for Molecular Beacon (MB) and Corresponding Linear Probes (LP) in the Absence (SSP) or Presence of Complementary or Centrally Mismatched DNA/RNA Targets[a]

			+DNA[b]				+RNA[b]				
	T_m		T_m	ΔT_m			T_m	ΔT_m	Φ_F		
probe	SSP	**B** =	G	A	C	T	G	C	SSP	+DNA	+RNA
DNA LP	–		57.0	−15.0	−14.5	−15.0	62.5	−13.5	0.17	0.74	0.85
DNA MB	55.0		56.0	−24.0	−24.5	−25.0	63.5	−17.5	0.15	0.55	0.62
O2′-Me RNA LP	–		59.0	−17.0	−19.0	−17.0	76.5	−15.5	0.15	0.68	0.74
O2′-Me RNA MB	66.0		46.0	–	−17.0	–	75.0	−29.0	0.17	0.45	0.61
DNA LP ref	–		46.0	−13.0	−14.0	−10.5	47.0	−14.0	–	–	–
DNA MB ref	50.0		46.5	−28.5	−28.5	−26.5	47.0	−16.0	–	–	–

[a] For sequences of modified probes see Table 1. **DNA LP ref** = 5′-[DNA]-(CCT TTA TCT GTT GCT); **DNA MB ref** = 5′-[DNA]-(C GCT CGA CCT TTA TCT GTT GCT TCG AGC G). The underlined region denotes target binding region. Conditions as described in Table 2, except that 0.5 μM of each strand was used; quantum yields were determined at 5 °C. "–" signifies not determined. [b] DNA targets: 3′-d(GGA AAT A**B**A CAA CGA). RNA targets: 3′-r(GGA AAU A**B**A CAA CGA).

The above results clearly demonstrate that it is possible to modulate and improve hybridization and fluorescence properties of 2′-*N*-(pyren-1-yl)carbonyl-2′-amino-LNA probes by alterations in backbone chemistry. Stimulated by this, our initial observations demonstrating that linear DNA probes with four separated Glowing LNA monomers are efficient hybridization probes,[47] and previous work on quencher-free MBs, we set out to generate long multilabeled linear probes and quencher-free MBs using monomer **X** (Figure 2). Four **X** monomers were incorporated as next-nearest neighbors into the 15-nt target recognition loop of a 29-mer MB composed of either a DNA or O2′-Me RNA backbone (**DNA MB** and **O2′-Me RNA MB**, Table 1). We hypothesized that low fluorescence levels would be observed in the absence of targets (**X** monomers in single-stranded region), while duplex formation with complementary DNA/RNA would result in intense fluorescence (pyrene moiety of monomer **X** pointing into the minor groove). The corresponding 15-mer linear probes (LPs), i.e., probes without the 7-bp stem (**DNA LP** and **O2′-Me RNA LP**), were synthesized to evaluate the influence of probe architecture on hybridization and fluorescence properties (Table 1).

DNA MB and **O2′-Me RNA MB** exhibit T_m values of 55.0 and 66.0 °C, corresponding to denaturation of the stem (Table 4; Figure S17, Supporting Information). The corresponding duplexes with DNA/RNA targets display smooth sigmoidal transition curves with T_m values ranging from comparable to markedly higher than those observed for the unmodified MB **DNA MB ref** (Table 4; Figure S18, Supporting Information). As expected from studies on conventional MBs,[63] **DNA MB** and **O2′-Me RNA MB** display similar or increased thermal mismatch discrimination relative to their corresponding linear probes (Table 4). The improved discrimination of a centrally C:C-mismatched RNA target by **O2′-Me RNA MB** (ΔT_m = −29.0 °C) is particularly remarkable and is in agreement with the observations with **O2′-Me RNA 2X** (Table 3).

As hypothesized, low fluorescence quantum yields were observed in the absence of DNA/RNA targets for **LP** and **MB** probes (SSP), while hybridization of **LP** or **MB** probes to DNA/RNA targets results in the formation of brightly fluorescent duplexes with very high quantum yields (Table 4). Accordingly, between 4- and 11-fold increases in fluorescence intensity were observed upon hybridization to complementary DNA/RNA, which constitutes the first example of multilabeled quencher-free MBs (Figure 6; Figures S19−22, Supporting Information). Greater increases were typically observed (a) with linear probes and (b) upon hybridization with RNA targets.

As a proof of concept, we set out to demonstrate detection of specific mRNA in cell culture studies using quencher-free MBs. The recognition loop of **DNA MB** and **O2′-Me RNA MB** targets the mRNA (bases 1164−1178, Figure S24, Supporting Information) of component X (Pdhx)[64,65] of the mouse pyruvate dehydrogenase complex (PDC).[66,67] Pdhx maintains the integrity of PDC, which is a key multiprotein complex that catalyzes the oxidative decarboxylation of pyruvate into Acetyl-CoA. Given the important role of PDC in cellular respiration (links glycolysis with Krebs cycle), Pdhx is abundantly present in cells and serves as a good model target for evaluation of quencher-free MBs modified with 2′-*N*-(pyren-1-yl)carbonyl-2′-amino-LNA monomer **X**.

First, the binding specificity of **DNA MB** was assessed using an *in vitro* transcription assay. Linearized plasmids, containing a partial cDNA sequence of Pdhx (441 bp) that encompasses the target region of the **MB** probes, were transcribed *in vitro* using either SP6 or T7 RNA polymerase to furnish sense (S) or antisense (AS) mRNA, respectively (see Supporting Information). Incubation of a constant excess amount of **DNA MB** with varying amounts of target AS-mRNA furnished a clear, dose-dependent increase in fluorescence intensity, whereas incubation with nontarget S-mRNA resulted in much smaller increases (Figure 7). This strongly suggests that binding between **DNA MB** and mRNA is occurring at conditions that closely mimic physiological conditions[68]—lack of binding between **DNA MB** (present in excess) and mRNA would otherwise have resulted in constant low fluorescence intensity.

Next, murine 3T3-L1 cells grown in 24-well plates on glass coverslips were transfected with MBs using Lipofectamine 2000, fixed by formaldehyde treatment, mounted on glass slides, and analyzed using fluorescence plate readers and/or fluorescence microscopy (see Supporting Information). As anticipated, a dose−response study using **DNA MB** revealed linearly increasing cellular fluorescence intensity with increasing concentrations of probe (Figures S25−S27, Supporting Information). [The brightness of the observed fluorescence is remarkable, considering that cells were observed using suboptimal emission filter

(63) Bonnet, G.; Tyagi, S.; Libchaber, A.; Kramer, F. R. *Proc. Natl. Acad. Sci. U.S.A.* **1999**, *96*, 6171–6176.
(64) Neagle, J. C.; Lindsay, J. G. *Biochem. J.* **1991**, *278*, 423–427.
(65) Lawson, J. E.; Behal, R. H.; Reed, L. J. *Biochemistry* **1991**, *30*, 2834–2839.
(66) Holness, M. J.; Sugden, M. C. *Biochem. Soc. Trans.* **2003**, *31*, 1143–1151.
(67) Behal, R. H.; Buxton, D. B.; Robertson, J. G.; Olson, M. S. *Annu. Rev. Nutr.* **1993**, *13*, 497–520.
(68) Krieg, P. A.; Melton, D. A. *Nucleic Acids Res.* **1984**, *12*, 7057–7070.

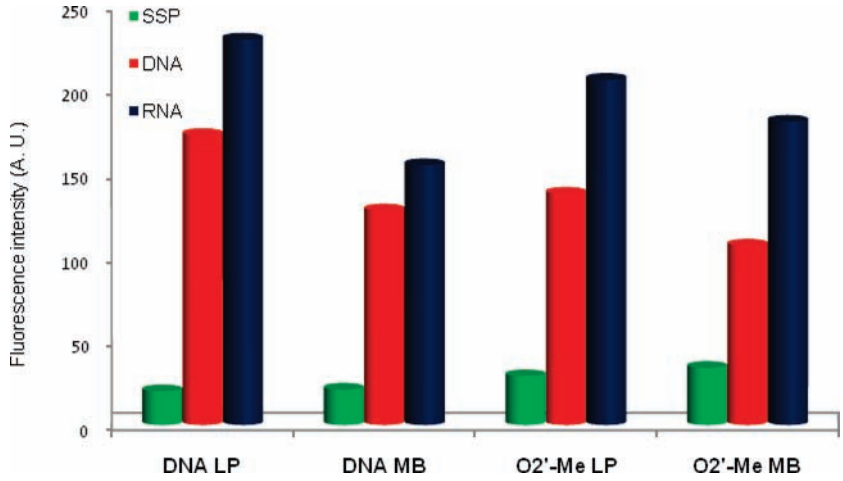

Figure 6. Fluorescence intensity of linear probes (LPs) and molecular beacons (MBs) in the absence (SSPs) or presence of complementary DNA or RNA. $\lambda_{ex} = 340$ nm, $\lambda_{em} = 402$ nm (**DNA LP** and **DNA MB**) and 405 nm (**O2′-Me LP** and **O2′-Me MB**), $T = 25$ °C.

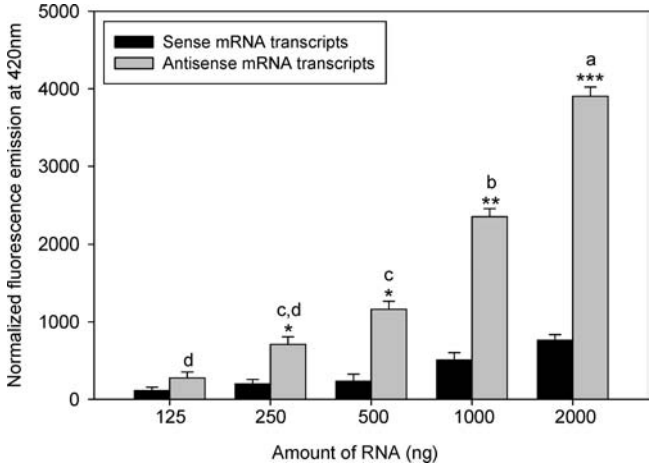

Figure 7. Detection of *in vitro* transcribed antisense (target) or sense (nontarget) mRNA by **DNA MB**. Varying amounts of RNA transcripts were incubated with 500 ng of DNA MB. Fluorescence emission ($\lambda_{ex} = 355$ nm, $\lambda_{em} = 420$ nm) was normalized to that of the control (0 ng of RNA). Data are means ± SE ($n = 3$). Different letters represent statistical significance of absolute differences of fluorescence emitted by sense and antisense transcripts at each dose ($P < 0.05$). Asterisks represent statistical differences in pairwise comparisons of fluorescence emission values between sense and antisense transcripts at each dose:* represents $P < 0.01$, ** represents $P < 0.001$, and *** represents $P < 0.0001$).

settings.] Transfection of negative control sequences established that cellular (auto)fluorescence is not observed at these conditions (*vide infra*).

Next, a time-course study with **DNA MB** revealed that the fluorescence signal from probe−target complexes (a) remained highly intense throughout different time points (16−48 h post transfection), indicating high probe biostability, and (b) appeared to accumulate in the perinuclear region (Figure S28, Supporting Information). [The influence of **DNA MB** and **O2′-Me RNA MB** on mRNA levels is discussed in the Supporting Information (Figure S29).] Although this coincides with the cellular location at which mRNA-templated protein synthesis occurs, additional studies are needed to confirm the precise subcompartment from which the fluorescence signal arose. Finally, a comparative study was performed between **DNA MB** and **O2′-Me RNA MB** to evaluate the influence of backbone chemistry on the cellular imaging characteristics of these quencher-free MBs. Visual inspection (Figure 8) as well as quantification of fluorescence

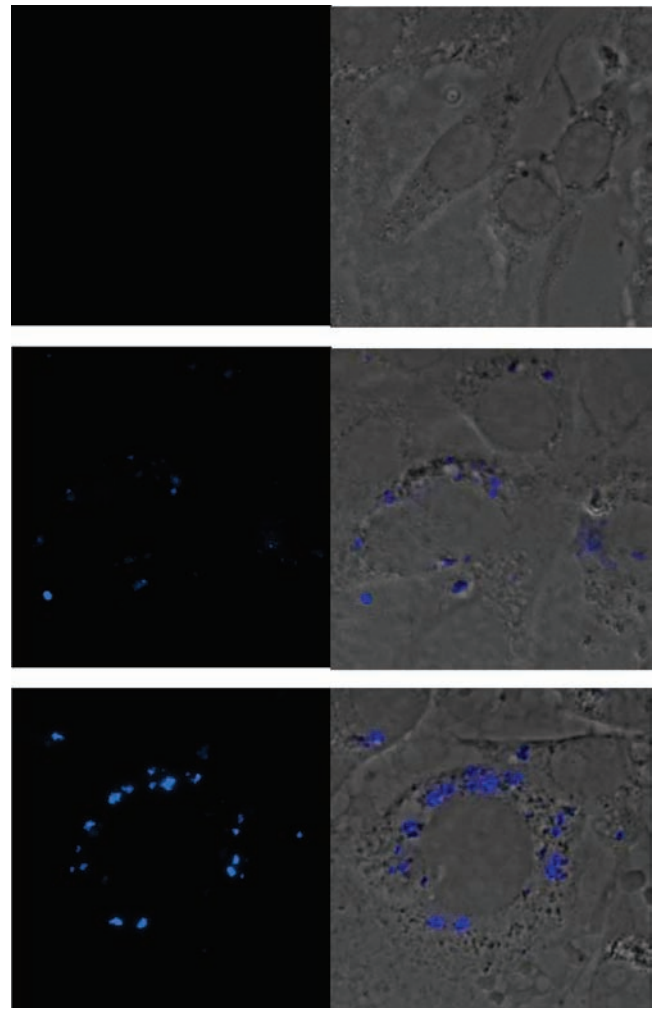

Figure 8. Photomicrograph images of 3T3-L1 cells treated with a negative control MB (top panel), **DNA MB** (middle panel), or **O2′-Me RNA MB** (lower panel). Fluorescence emission (filter settings: $\lambda_{ex} = 340-380$ nm, dichroic mirror allowing passage of $\lambda > 400$ nm, and $\lambda_{em} = 435-485$ nm) was observed at 24 h post transfection by fluorescence microscopy at 60× and represented as the fluorescent image (left) and as an overlay of fluorescent image and transmitted light image (right). Images are 50 μm across.

signals (Figure S30, Supporting Information) clearly demonstrates that cells treated with **O2′-Me RNA MB** exhibit much

stronger fluorescence emission than cells treated with **DNA MB**, while MBs designed as negative controls did not exhibit noticeable fluorescence. This most likely reflects higher affinity and biostability of **O2′-Me RNA MB** as compared to **DNA MB**, although differential cellular uptake and/or compartmentalization cannot be ruled out. Interestingly, fluorescence again appeared to accumulate in the perinuclear region, providing additional support to the notion that Glowing LNAs are capable of visualizing cellular mRNA near the site of protein synthesis. In addition, these constructs have apparently low cytotoxicity (results not shown), providing an excellent approach to investigation of specific cellular physiology that is minimally disruptive to cellular processes.

Conclusion

The present study demonstrates that hybridization and fluorescence properties of *Glowing LNA* probes can be efficiently modulated by changes in backbone chemistry and probe architecture. Multilabeled Glowing LNA probes with O2′-Me RNA backbones exhibit (a) high affinity toward RNA targets, (b) excellent mismatch discrimination that can be additionally improved using a quencher-free molecular beacon design, (c) high biostability, and (d) pronounced hybridization-induced increases in fluorescence intensity leading to formation of brightly fluorescent duplexes with emission quantum yields that are unprecedented among pyrene-labeled oligonucleotides. These characteristics enabled detection of mRNA in (a) *in vitro* transcription assays and (b) both quantitative fluorometric assays and direct microscopic observation of probes bound to mRNA in its native form (in living cells). The results suggest that multilabeled quencher-free molecular beacons modified with 2′-*N*-(pyren-1-yl)carbonyl-2′-amino-LNA monomer **X** constitute a new probe paradigm for detection of mRNA. Additional studies using a variety of mRNA targets and cell lines must be performed to fully evaluate the seemingly bright potential of Glowing LNA probes.

Acknowledgment. This article is dedicated to Prof. Leszek Czuchajowski (Dept. Chemistry, University of Idaho) in celebration of his 85th birthday. Financial support from Idaho NSF EPSCoR (P.J.H.), the BANTech Center at University of Idaho (P.J.H., R.A.H.), and a scholarship from the College of Graduate Students, University of Idaho (M.E.Ø.) is greatly appreciated. Input from Prof. Jesper Wengel (Nucleic Acid Center, University of Southern Denmark) and assistance from Dr. B. Ravindra Babu, Mr. Troels Jensen, Ms. K. Østergaard, Ms. S. L. Wengel (all Nucleic Acid Center, University of Southern Denmark), and Ms. B. M. Dahl (University of Copenhagen) during preparation of monomers and oligonucleotides are sincerely valued.

Supporting Information Available: Protocols for synthesis and purification of ONs, recording of thermal denaturation curves and steady-state fluorescence emission spectra, and determination of quantum yields; representative thermal denaturation profiles; additional data for mismatched duplexes (T_m values and fluorescence emission spectra); kinetics of MBs; cell culture conditions; transfection of MBs into cells; *in vitro* transcription; dose−response and time course studies; and Pdhx gene expression analysis. This material is available free of charge via the Internet at http://pubs.acs.org.

JA1057295